Rituximab antiproliferative effect in B-lymphoma cells is associated with acid-sphingomyelinase activation in raft microdomains

Christine Bezombes, Solène Grazide, Céline Garret, Claire Fabre, Anne Quillet-Mary, Sabina Müller, Jean-Pierre Jaffrézou, and Guy Laurent

Rituximab is a chimeric human immunoglobulin G1 (IgG1) anti-CD20 monoclonal antibody with significant activity against CD20$^+$ malignant B cells. Rituximab is currently used with success in the treatment of B-cell–derived lymphoid neoplasias either alone or in combination with chemotherapy. However, the predominant mechanism by which rituximab exerts its antitumor properties in vivo remains unknown. In the present study, we demonstrate that in Daudi and RL B-lymphoma cells, rituximab (without cross-linking) used at the saturating dose of 10 μg/mL induced moderate accumulation in G_1 phase, growth inhibition, and significant loss in clonogenic potential. However, in these cells, rituximab induced no apoptosis. Furthermore, we observed that treatment with rituximab resulted in a rapid and transient increase in acid-sphingomyelinase (A-SMase) activity and concomitant cellular ceramide (CER) generation in raft microdomains. We also observed that rituximab-treated cells externalized both A-SMase and CER that colocalized with the CD20 receptor. Finally, we present evidence that rituximab-induced growth inhibition may be mediated through a CER-triggered signaling pathway, leading to the induction of cell cycle–dependent kinase inhibitors such as p27(Kip1) through a mitogen-activated protein kinase (MAPK)–dependent mechanism. (Blood. 2004;104: 1166-1173)

Introduction

Rituximab is a chimeric human immunoglobulin G1 (IgG1) anti-CD20 monoclonal antibody with significant activity against CD20$^+$ malignant B cells. Rituximab is currently used with success in the treatment of B-cell–derived lymphoid neoplasias either alone or in combination with chemotherapy. The predominant mechanism by which rituximab exerts its antitumor properties in vivo remains debated. However, in vitro studies suggest that complement-mediated cytotoxicity or antibody-dependent cell-mediated cytotoxicity could play an important role. It has been also shown, at least in some malignant B cells, that rituximab may exert apoptotic or antiproliferative effects.[1] Nevertheless, it has been established that this antibody induces only modest levels of apoptosis unless it is cross-linked with antihuman immunoglobulin, whereas treatment with rituximab without cross-linker results in reduced cell growth kinetics.[2] Although rituximab's antiproliferative effect has been minimized compared with apoptosis, the fact that responding patients generally displayed progressive tumor mass reduction and that complete response is usually achieved several weeks after completion of therapy suggests that, in vivo, cell growth inhibition could play a more important role than apoptosis which rather implies rapid tumor cell disintegration.

The effect of rituximab on cell growth suggests that this antibody activates CD20-coupled signaling pathways, resulting in the production of second messengers, which, in turn, could interfere with cell-cycle control. Indeed, previous studies have established that, once activated by rituximab, CD20 molecules are redistributed to raft microdomains and that interaction between CD20 and raft membrane protein components results in the activation of the transmembrane signaling machinery (reviewed in Deans et al[3]). CD20-associated raft proteins include Src-family members such as Lyn, Fyn, and Lck, as well as p75/80 (Cbp/PAG), a tyrosine phosphorylated protein, which acts in concert with Lyn.[4] These tyrosine phosphorylation events play an important role in mediating downstream effector signaling pathways. Among these pathways, it has been proposed that the activation of the mitogen-activated protein kinase p38MAPK is critical for the inhibitory effect of rituximab.[5] However, the mechanisms that link transmembrane signaling, MAPK activation, and growth inhibition remain unknown.

We raised the possibility that ceramide (CER), a lipid second messenger, may contribute to the propagation of CD20-mediated signaling toward growth inhibition through MAPK. Indeed, CER has emerged as not only a potent apoptosis inducer (reviewed in Pettus et al[6]) but also a negative regulator of cell growth through modulation of cell-cycle regulators, including p21(WAF-1) and p27(Kip1).[7,8] In addition, CER regulates MAPK, not only extracellular signal-regulated kinase (ERK) and c-jun NH2-terminal protein kinase (JNK) but also p38MAPK.[9-11] Moreover, CER has been involved in apoptosis induced by anti-immunoglobulin or through

From the Institut National de la Santé et de la Recherche Médicale U563-CPTP, Centre Hospitalier et Universitaire Purpan Pavillon Lefebvre, Toulouse, France; and the Service d'Hématologie, Centre Hospitalier Universitaire Purpan, Toulouse, France.

Submitted January 23, 2004; accepted April 13, 2004. Prepublished online as *Blood* First Edition Paper, May 11, 2004; DOI 10.1182/blood-2004-01-0277.

Supported by la Ligue Nationale Contre le Cancer and les Comités Départementaux de l'Aude, de l'Aveyron, du Cantal, et de la Haute-Garonne (J.P.J), and la Faculté de Médecine Toulouse-Rangueil (G.L.), as well as grants from l'Association pour la Recherche sur le Cancer (C.B.) and la Fondation pour la Recherche Médicale (S.G.).

C.B. and S.G. contributed equally to this work.

Reprints: Christine Bezombes, INSERM U563, CPTP, CHU Purpan, Pavillon Lefebvre, 31024 Toulouse Cedex, France; e-mail: christinebezombes@yahoo.com.

The publication costs of this article were defrayed in part by page charge payment. Therefore, and solely to indicate this fact, this article is hereby marked "advertisement" in accordance with 18 U.S.C. section 1734.

B-cell receptor (BCR) activation, suggesting that this mediator is functional in B cells.[12,13]

CER can be generated through different metabolic routes in the cell. First, sphingomyelin (SM) hydrolysis on activation of either neutral or acid sphingomyelinase (N-SMase or A-SMase), which results in the release of CER and phosphocholine.[14] Second, CER can be issued from de novo synthesis because of the stimulation of serine palmitoyl transferase and/or CER synthase. Both of these pathways have been implicated in the cellular response to stress induced by genotoxic agents, radical oxygen species, and activation of death receptors, including Fas, p55 tumor necrosis factor (TNF) receptor, and p75 neurotrophin receptor.

In this study, we have investigated whether rituximab may influence CER metabolism in malignant B cells, and the possible consequences of altered CER metabolism on MAPK activity, cell-cycle control, and cell growth.

Materials and methods

Drugs and reagents

Rituximab and alemtuzumab (Campath-1H) were kindly provided by Roche (Hertfordshire, United Kingdom) and Schering (Lille, France) laboratories, respectively. Silica gel 60 thin-layer chromatography plates were from Merck (Darmstadt, Germany). All other drugs and reagents were purchased from Sigma Chemical (St Louis, MO), Alexis Biochemicals (Paris, France), Matreya Biochemicals (Marne-La-Vallée, France), Carlo Erba (Rueil-Malmaison, France), or Prolabo (Paris, France). SR33557 was kindly provided by Dr J.M. Herbert (Sanofi-Synthélabo, Toulouse, France).

Cell culture

Daudi cells are Burkitt lymphoma cells, whereas RL cells are follicular lymphoma cells carrying the t(14;18). Daudi and RL cells were obtained from ATCC (Rockville, MD) and cultured in RPMI 1640 medium at 37°C in 5% CO_2. Culture medium was supplemented with 10% heat-inactivated fetal calf serum (FCS), complemented with 2 mM L-glutamine, 200 U/mL penicillin, and 100 μg/mL streptomycin (all from Eurobio, Les Ulis, France). Chronic lymphocytic leukemia (CLL) cells were collected from peripheral blood of patients with CLL after informed consent and separated by Ficoll-Hypaque density gradient. For each sample, flow cytometry analysis revealed that CLL cells displayed a common $CD19^+$ $CD5^+$ B-CLL phenotype.

Saturating concentration determination

After a wash in phosphate-buffered saline (PBS) containing 1% FCS, Daudi and RL cells were incubated at 4°C for 30 minutes in presence of rituximab at various concentrations or irrelevant human IgG (10 μg/mL). After 2 washes in PBS containing 1% FCS, cells were incubated with a peroxidase-conjugated goat antihuman IgG antibody for 30 minutes at 4°C. Fluorescence intensities were evaluated by using flow cytometry (FACScan; Becton Dickinson, Pont-de Claix, France). Saturating concentration of rituximab was obtained from the fluorescence difference (ΔFL2) between rituximab- and IgG-treated cells.

Clonogenic assay

Cells were treated with rituximab (10 or 50 μg/mL), suspended in completed medium (100 μL), and seeded on 96-well plates (50 cells/well) to determine the cell colony formation. After 7 days, the colony number was determined under an inverted microscope, and the percentage of survival was determined.

Cell cycle analysis

One million cells were permeabilized with ethanol 80% and stored at −80°C during 2 hours. Cells were then washed, resuspended in propidium iodide (50 μg/mL), and treated for 30 minutes at room temperature with 0.1 mg/mL RNAse A. Cell cycle analysis was performed by flow cytometry using a Lysis II program on a FACScan (Becton Dickinson, San Jose, CA).

Cell viability

Exponentially growing cells were treated or not with various concentrations of C_{16}-ceramide, and viability was evaluated after a time course by counting cells using trypan blue exclusion.

Reversibility assay

Exponentially growing cells were treated or not with 10 μg/mL rituximab during 24 hours and then treated or not with 0.4% *Streptomyces griseus* protease (Type XXI; Sigma, St Louis, MO). The reversibility of the biologic effect of rituximab was evaluated by counting cells using trypan blue exclusion.

Isolation of membrane microdomains

Rafts were isolated from cells as previously described.[15] For each isolation, 100×10^6 cells were washed twice with PBS. After treatment with or without the appropriate drugs, cells were pelleted by centrifugation, resuspended in 1 mL ice-cold MBS-buffered saline (150 mM NaCl, 25 mM 2-(*N*-morpholino)-ethanesulfonic acid, pH 6.5) containing 1% (wt/vol) Triton X-100. After 30 minutes on ice, cells were further homogenized by 10 strokes of a Dounce homogenizer on ice. Ice-cold MBS (1.5 mL) was added, and 2 mL of this suspension was mixed with 2 mL of 80% (wt/vol) sucrose in MBS. This mixture was subsequently loaded under a linear gradient consisting of 8 mL 5% to 40% (wt/vol) sucrose in MBS. All solutions contained the following protease inhibitors: 100 μM phenylmethylsulfonylfluoride; 1 mM EDTA (ethylenediaminetetraacetic acid); and 1μM each of aprotinin, leupeptin, and pepstatin A. Gradients were centrifuged in a Beckman SW 41 swinging-rotor (Beckman Coulter, Roissy, France) at 260/809*g* for 20 hours at 4°C. Twelve fractions of 1 mL each were collected (from top to bottom), mixed by vortex, and stored at −80°C. The protein content of both fractions and the total initial cell suspension was measured using bovine serum albumin (BSA) as standard.[16]

Cholesterol depletion and repletion

For cholesterol depletion, cells were incubated in RPMI 10% FCS containing 10 mM methyl-β-cyclodextrin for 20 minutes at 37°C and then used for fluorescence-activated cell sorting (FACS) analysis.

For cholesterol repletion, cholesterol-depleted Daudi cells were centrifuged and resuspended for 30 minutes at 37°C in RPMI 10% containing cholesterol/methyl-β-cyclodextrin complexes: cholesterol (200 μL) in $CHCl_3/CH_3OH$ (1/2 vol/vol) was added to a final concentration of 2 mM in 10 mL RPMI 10% FCS containing 5 mM methyl-β-cyclodextrin while stirring at 80°C. The solution was homogenized by sonication (60 kHz, 3×20 seconds), filtered through a 0.2-μm (VWR, Strasbourg, France), and then maintained at 37°C. Cells were washed and used for FACS analysis.

A-SMase and N-SMase assays

On whole cells. A-SMase activity was assayed as previously described by using [choline-methyl-^{14}C]SM (120 000 dpm/assay; NEN, Paris, France).[17,18]

On raft fractions. Pooled fractions (250 μL aliquot) were assayed for the presence of different SMase activities.[17] Reactions were started by adding 250 μL substrate solution that consisted of [^{14}C-methylcholine]SM (1×10^5 dpm/assay; DuPont-NEN, Boston, MA), 0.1% (wt/vol) Triton X-100, and 10 mM EDTA in 200 mM sodium acetate buffer (pH 5.0). After a 2-hour incubation at 37°C, reactions were terminated by adding 2.5 mL chloroform/methanol (2:1, vol/vol). Phases were separated by centrifugation (1000*g*, 10 minutes), and the amount of released radioactive phosphocholine was determined by subjecting 750 μL of the upper phase to scintillation counting.

The amount of radiolabeled substrate that was hydrolyzed during an assay never exceeded 10% of the total amount of substrate added. For calculation of the specific activities in total cell homogenates, values were corrected for protein content, reaction time, and specific activity of the substrate.

Metabolic cell labeling and sphingolipid quantitation

Total cellular CER quantitation was performed by labeling cells to isotopic equilibrium with 1 μCi/mL (0.037 MBq) [9, 10-^{3}H]palmitic acid (53.0 Ci/mmol [196.1 × 10^{10} Bq/mmol]; Amersham Pharmacia Biotech, Orsay, France) for 48 hours in complete medium as previously described.[16] Cells were then washed and resuspended in complete medium for time course experiments. Lipids were extracted and resolved by thin-layer chromatography; CER was scrapped and quantified by liquid scintillation spectrometry.

SM quantitation was performed by labeling cells to isotopic equilibrium with 0.5 μCi/mL (0.0185 MBq) [methyl-^{3}H]choline (81.0 Ci/mmol [299.7 × 10^{10} Bq/mmol]; Amersham Pharmacia Biotech) for 48 hours in complete medium.[17-19] Cells were then washed and resuspended in complete medium for kinetic experiments. Radiolabeled SM was extracted and quantified by scintillation counting.

Total cellular CER quantitation in fresh B cells was performed using *Escherichia coli* diacylglycerol kinase (Amersham, Buckinghamshire, United Kingdom) according to previously published procedures.[20]

FACS analysis

Cells were incubated with or without 10 μg/mL rituximab, fixed for 10 minutes in 4% paraformaldehyde (PFA) (wt/vol) in PBS. Cells were then washed and further incubated for 45 minutes with a rabbit polyclonal anti–A-SMase (Santa Cruz Biotechnology, Santa Cruz, CA) or mouse monoclonal anti-CER 15B4 (Alexis, Coger, Paris, France). Cells were then washed in PBS containing 1% heat-inactivated FCS, and stained for 45 minutes with fluorescein isothiocyanate (FITC)–labeled goat antirabbit or antimouse (Jackson ImmunoResearch Laboratories, Baltimore, PA). After a final PBS wash, cells were analyzed on a fluorescence-activated cell sorter (FACScalibur; Becton Dickinson, Le Pont du Claix, France).

Confocal microscopy

Cells were incubated with or without 10 μg/mL rituximab for 15 minutes, fixed for 10 minutes in 4% PFA (wt/vol) in PBS, permeabilized or not for 10 minutes with 0.1% saponin in PBS containing 3% bovine serum albumin (wt/vol) and 1 mM HEPES (*N*-2-hydroxyethylpiperazine-*N*′-2-ethanesulfonic acid) (PBS-BSA). Cells were then washed and further incubated for 45 minutes with a rabbit polyclonal anti–A-SMase or with a mouse monoclonal anti-CER 15B4. Cells were then washed in PBS-BSA and stained for 45 minutes with FITC-labeled goat antirabbit, with Cy3-labeled goat antimouse, or with Cy5-labeled mouse anti–human Fc. After a final PBS-BSA wash, cells were mounted on glass coverslips with Dako mounting medium (Dako, Trappes, France). Slides were examined with a Carl Zeiss Axiovert 200 confocal microscope (Carl Zeiss, Oberkochen, Germany) using a 63 × Plan-Apochromat objective (1.4 oil). An argon laser at 488 nm was used to excite FITC (emission 515-540 nm), and a helium-neon laser was filtered at 633 nm to excite Cy5 (emission 680 nm) regulated by LSM 510 software (Zeiss). Control staining was performed with secondary antibodies alone. For raft microdomain labeling, cells were incubated with FITC-cholera toxin for 15 minutes at 4°C prior to fixation with PFA. Cholera toxin, which binds GM1, a major lipidic component of rafts, allows these microdomains to be detected.

Western blot analysis for ERK and p27(Kip1)

Five million exponentially growing cells treated or not with rituximab (10 μg/mL) were washed in PBS, centrifuged, and lysed in the sodium dodecyl sulfate (SDS) sample buffer containing 62.5 mM Tris (tris-(hydroxymethyl)aminomethane) pH 6.8, 2% wt/vol SDS, 10% glycerol, 50 mM DTT (dithiothreitol), and 0.01% wt/vol bromophenol blue. Cell lysates were then sonicated for 10 to 15 seconds. Sample (20 μL) was heated for 5 minutes at 95°C, loaded onto 10% (wt/vol) SDS–polyacrylamide gel electrophoresis (PAGE), and transferred electrophoretically onto nitrocellulose membranes (Hybond-C; Amersham Pharmacia Biotech). Nonspecific binding sites were blocked in 10 mM Tris-buffered saline (TBS) containing 0.1% Tween-20, 10% nonfat milk. Membranes were then incubated overnight at 4°C with anti-ERK (Santa Cruz Biotechnology), antiphospho p44/42 MAPK, or anti-p27(Kip1) (Cell Signaling Technology, Beverly, MA) antibodies. Membranes were then washed 3 times at room temperature, and bound immunoglobulin was detected with secondary antibodies coupled to horseradish peroxidase (Beckman-Coulter, Roissy, France). The signal was visualized by enhanced chemiluminescence (ECL; Amersham Pharmacia Biotech) and autoradiography.

Statistics

Quantitative experiments were analyzed by using Student *t* test. All *P* values resulted from the use of 2-sided tests.

Results

Effect of rituximab on lymphoma B-cell growth

In Daudi cells, rituximab, at the saturating dose of 10 μg/mL, induced an inhibition of the cell growth as measured by trypan blue exclusion assay (Figure 1, Ai). To reinforce CD20 specificity, we

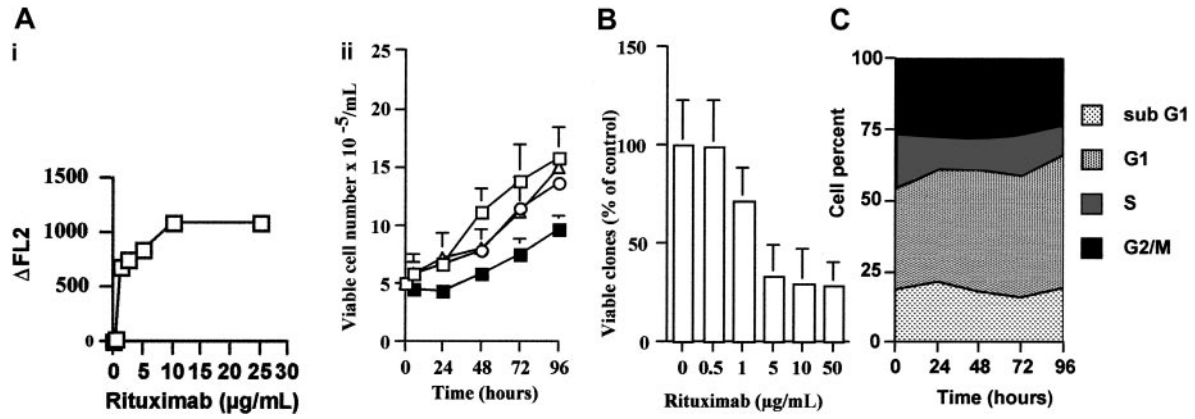

Figure 1. Rituximab induces cell growth inhibition. (A) Daudi cells (3 × 10^6) were either untreated (□) or incubated with rituximab (■), an irrelevant IgG (○), or alemtuzumab (△), all at 10 μg/mL. At various time points, cell number was estimated by trypan blue exclusion assay. Results are mean of triplicate determinations and are representative of 3 independent experiments. (Ai) Determination of rituximab saturation concentration. Aliquots of Daudi cells were incubated at 4°C for 30 minutes in the presence of various concentrations of rituximab or an irrelevant human IgG (10 μg/mL). Saturating concentration of rituximab (10 μg/mL) was obtained from the fluorescence difference (ΔFL2) between rituximab- and IgG-treated cells as described in "Materials and methods." (B) Clonogenic assay. Daudi cells were either untreated or treated with rituximab at 0.5, 1, 5, 10, or 50 μg/mL. After 7 days, the number of colonies was determined under an inverted microscope, and the percentage of survival was determined. Results are mean of triplicate determinations ± SD. (C) Cell cycle analysis. Daudi cells were treated with 10 μg/mL rituximab, and cell distribution into the cell cycle was performed as described in "Materials and methods." Results are representative of 3 independent experiments.

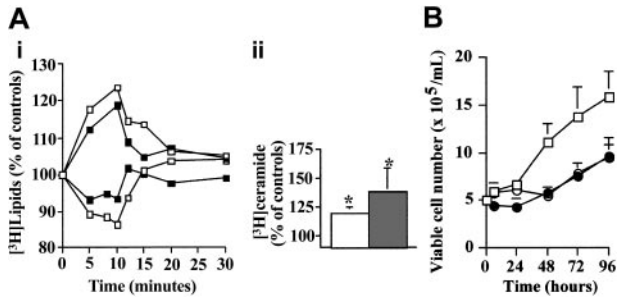

Figure 2. CER generation and SM hydrolysis in B cells. (Ai) Rituximab induces CER generation and SM hydrolysis in B cells. Daudi (□) and RL (■) cells were prelabeled with [9, 10-^{3}H] palmitic acid or [methyl-^{3}H]choline to equilibrium for 48 hours and then treated with 10 μg/mL rituximab for various time points. After which, both tritiated CER (top line) and SM (bottom line) levels were quantitated as described in "Materials and methods." Results are representative of 3 independent experiments. (Aii) Mean of peak CER levels obtained from 3 independent experiments. *$P < .01$. (B) Effect of fumonisin B1 on cell viability. Daudi cells were preincubated (●) or not (○, □) 24 hours with 25 μM fumonisin B1 and then treated (○, ●) or not (□) with 10 μg/mL rituximab. Cell number was estimated by trypan blue exclusion assay. Results are the mean of 3 independent experiments ± SD.

tested another chimeric antibody (anti-CD52, alemtuzumab) and a nonimmune IgG fraction. Neither alemtuzumab monoclonal antibody (MoAb; 10 μg/mL) nor IgG (10 μg/mL) influenced cell growth (Figure 1Aii). Similar results were obtained from RL cells (data not shown). The inhibitory effect of rituximab was also evaluated by clonogenic assay. As shown in Figure 1B, we found that rituximab induced a dose-dependent reduction of colony formation in Daudi cells with a maximum of 5 to 10 μg/mL. Similar results were obtained with RL cells (data not shown). The influence of rituximab on cell cycle distribution was performed with propidium iodide/bromodeoxyuridine double staining. Our experiments revealed that rituximab induced only a moderate accumulation in G_1 phase (Figure 1C), but no signs of apoptosis were observed as assessed by morphology and 4′, 6-diamidino-2-phenylindole, dilactate (DAPI) staining (data not shown).

The influence of time exposure of rituximab on cell growth inhibition was also investigated. In these experiments, Daudi cells coated with rituximab for 24 hours were treated with protease for 1 hour and then incubated for an additional period of 48 hours in antibody-free medium, and cell viability was measured by trypan blue exclusion assay. Proteolysis resulted in 79% ± 9% reduction of membrane-bound rituximab. However, cell growth inhibition was maintained, whereas treatment with protease alone did not affect cell viability (data not shown).

Altogether, these results suggested that, in Daudi cells, rituximab induced a CD20-mediated irreversible cell growth inhibition. Moreover, it appeared that rituximab's effect was completed within a short period of time, suggesting that the antibody triggered early molecular events, resulting in cell growth inhibition. Among these events, CER production was one of the possible candidates. For this reason, we examined the effect of rituximab on CER metabolism.

Effect of rituximab on intracellular CER concentration in B cells

Daudi and RL cells were prelabeled with [9, 10-^{3}H] palmitic acid or [methyl-^{3}H]choline to equilibrium for 48 hours and then treated with rituximab. In both cell lines, rituximab induced a rapid and transient CER generation that peaked at 5 to 10 minutes (Figure 2). Treatment with rituximab resulted in SM variations that mirrored CER concentration changes (Figure 2). It is important to note that the magnitude of SM loss and CER generation was comparable to that observed on stimulation by Fas, TNFα, p75NTR, and chemotherapeutic agents in other cellular models.[14] These results suggested that rituximab activated the SM cycle (ie, SM hydrolysis and resynthesis).

CER concentration was also monitored during a prolonged time period in Daudi cells to investigate whether rituximab could induce delayed CER generation. However, metabolic labeling revealed that the intracellular CER concentration remained stable over 96 hours (Figure 2B). Because delayed CER accumulation is generally associated with de novo synthesis,[21,22] this result suggested that rituximab had no effect on CER synthase. As a matter of fact, cotreatment with rituximab and fumonisin B1, a potent CER synthase inhibitor, had no influence on intracellular ceramide concentration (data not shown). Moreover, fumonisin B1 did not affect the inhibitory effect induced by rituximab on cell viability (Figure 2B). Altogether, these results suggested that, in rituximab-treated cells, CER production was mainly due to SM hydrolysis on stimulation of a SMase.

To confirm the influence of rituximab on CER metabolism in other B cells, we measured the variation of intracellular CER concentration in fresh leukemic B cells by using the diacylglycerol (DAG) kinase assay. Clinical characteristics of the patients are summarized in Table 1. DAG kinase assay revealed that, in rituximab-treated B-CLL cells, CER concentrations were increased, compared with untreated cells, in 6 of 8 samples. The fold-increase ranged from 13% to 80% of basal values.

Effect of rituximab on SMase activities in B cells

Because both N-SMase and A-SMase have been involved in CER production in cells treated with antitumor agents, we evaluated the activities of these enzymes in Daudi and RL cells treated with rituximab. These experiments showed that rituximab induced an increase in zinc-independent A-SMase activity within 5 to 10 minutes, thus correlating with CER release and SM hydrolysis (Figure 3A). However, N-SMase was unaffected (data not shown). Importantly, SR33557, a potent A-SMase inhibitor,[23] significantly abrogated not only A-SMase stimulation (Figure 3Bi) but also CER production induced by rituximab (Figure 3Bii). Similar results were obtained with perhexiline, another A-SMase inhibitor (data not shown).[24] Altogether, these results suggest that, in Daudi and RL cells, rituximab-induced activation of CD20 resulted in A-SMase stimulation is responsible for SM hydrolysis and subsequent CER production.

Effect of rituximab on A-SMase cellular localization

On the basis of previous studies which have documented that on death receptor–mediated A-SMase stimulation this enzyme translocates to the surface of the cell,[25-27] we investigated whether

Table 1. Characteristics of patients with B-CLL patients and CER production in rituximab-treated B-CLL cells

Patient	Age, y	Lymphocytosis, mm^3	Duration from diagnosis, y	Previous therapy	CER accumulation, %
1	80	38 600	0	No	+41
2	58	32 600	0.3	No	+75
3	60	82 000	0	No	+23
4	74	59 800	0	No	+36
5	66	30 600	4	CBL, CVP	NS
6	66	70 100	11	CBL, CVP	+80
7	75	19 100	11	CBL	+13
8	73	32 000	14	CBL	NS

Variation of intracellular CER concentration was assayed by using the DAG kinase assay. CBL indicates chlorambucil; CVP, cyclophosphamide, vincristine, prednisone; NS, not significant.

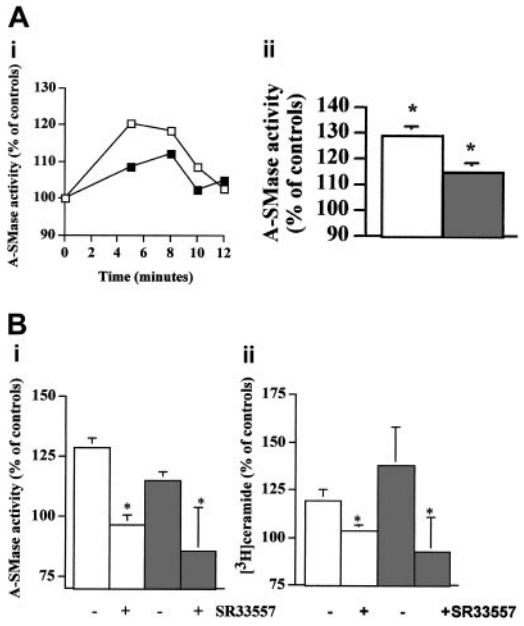

Figure 3. Inhibitory effect induced by rituximab is mediated by A-SMase activation-derived CER. (Ai) Activation of A-SMase by rituximab in B cells. Daudi (□) and RL (■) cells were treated with 10 μg/mL rituximab for various time points. After which, A-SMase activity was quantitated as described in "Materials and methods." Results are representative of 3 independent experiments. (Aii) Mean of peak A-SMase activation obtained from 3 independent experiments, ± SD. *$P < .01$. (B) Inhibition of rituximab-induced A-SMase activation and CER generation by SR33557. Daudi (□) and RL (■) cells were preincubated 1 hour with 30 μM SR33557 and then treated with 10 μg/mL rituximab for various time points. After which, both A-SMase activity (i) and CER levels (ii) were quantitated as described in "Materials and methods." Results are mean of peak A-SMase activation and CER obtained from 3 independent experiments, ± SD. *$P < .01$.

rituximab may induce A-SMase translocation from intracellular compartments to the external leaflet of the plasma membrane. As a matter of fact, confocal microscopy on permeabilized cells revealed that a subset of the intracellular A-SMase is redistributed toward the cell membrane, colocalizing with CD20 in rituximab-treated cells (Figure 4A). Flow cytometry analysis performed with anti–A-SMase antibody in intact cells revealed that treatment with rituximab resulted in A-SMase translocation to the plasma membrane in Daudi and RL cells (data not shown) as well as in B-CLL cells (sample from patient 1 in Figure 4B).

Effect of rituximab on CER cellular localization

On the basis of previous studies that have documented that on A-SMase translocation CER accumulates at the cell surface,[25-27] we investigated whether rituximab may induce CER accumulation at the external leaflet of the plasma membrane. Indeed, flow cytometry analysis using an anti-CER 15B4 antibody revealed that treatment with rituximab resulted in CER accumulation at the cell surface of intact Daudi cells (Figure 4C) and RL cells (data not shown) as well as in B-CLL cells (sample from patient 1 in Figure 4D). Positive controls were provided by CER immunolocalization using anti-CER 15B4 antibody in Daudi cells treated with bacterial SMase (0.2 U) (Figure 4E).

Effect of long chain C_{16}-CER on cell viability

To evaluate the possible role of rituximab-induced CER accumulation at the external surface of the plasma membrane on cell growth inhibition, we evaluated the effect of C_{16}-CER, a cell nonpermeant CER, on Daudi cell viability. As shown in Figure 4F, C_{16}-CER induced a concentration-dependent growth inhibitory effect, thus mimicking the effect of rituximab in these cells. This result suggests that CER accumulation at the cell surface mediates cell growth inhibition.

Membrane localization of rituximab-induced SM-CER pathway

Previous studies have described that rituximab induced CD20 redistribution to raft microdomains in malignant B cells.[4,28] On the basis of results presented in Figure 4, we investigated whether activated A-SMase colocalized with CD20. We first confirmed that rituximab (10 μg/mL; 15 minutes) induced a CD20 delocalization from heavy fractions to raft fractions in treated Daudi and RL cells (Figure 5A). Moreover, we found that in rituximab-treated cells, most A-SMase activity was contained into raft fractions (Figure 5B).

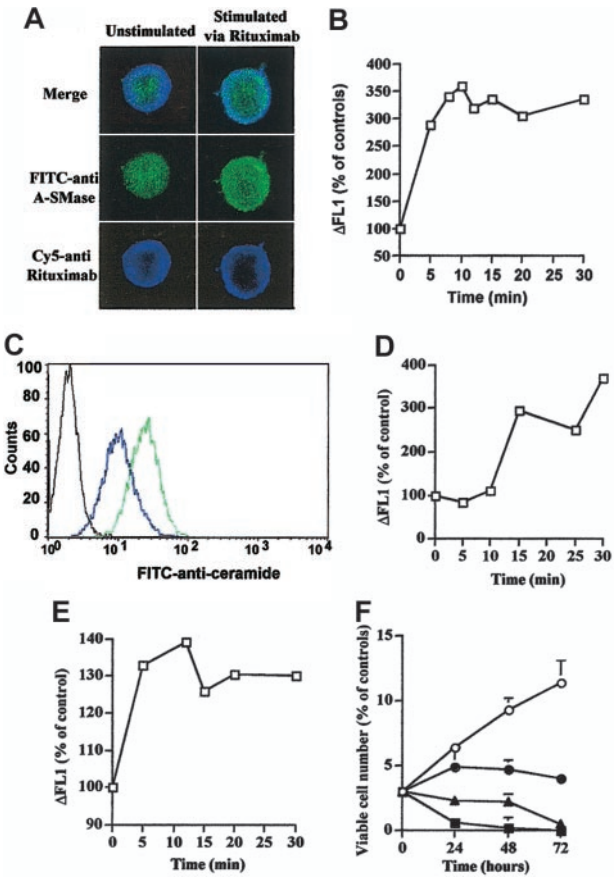

Figure 4. Rituximab induces A-SMase and CER localization in the outer leaflet of the cell membrane. (A) Cells (3×10^6) were treated with or without 10 μg/mL rituximab for 10 minutes and analyzed by confocal microscopy by using rabbit anti-SMase and/or mouse antihuman Fc. Results are representative of 3 independent experiments. (B) Rituximab induces outer leaflet A-SMase localization in B-CLL fresh cells. Intact cells (3×10^6) from patient 1 were treated or not with 10 μg/mL rituximab for 10 minutes and analyzed by flow cytometry using a FITC-labeled rabbit polyclonal anti–A-SMase. Results are representative of 3 independent experiments. (C) Intact cells (3×10^6) were treated (green line) or not (blue line) with 10 μg/mL rituximab for 10 minutes and analyzed by flow cytometry by using a FITC-labeled mouse monoclonal anti-CER 15B4. Results are representative of 3 independent experiments. A stained FITC anti-mouse served as control (black line). (D) Rituximab induces outer leaflet CER accumulation in B-CLL fresh cells. Intact cells (3×10^6) from patient 1 were treated or not with 10 μg/mL rituximab and analyzed by flow cytometry by using a FITC-labeled mouse monoclonal anti-CER 15B4. Results are representative of 3 independent experiments. (E) Bacterial SMase induces outer leaflet CER accumulation in Daudi cells. Intact cells (3×10^6) were treated or not with 0.2 U bacterial SMase and analyzed by flow cytometry by using a FITC-labeled mouse monoclonal anti-CER 15B4. Results are representative of 3 independent experiments. (F) C_{16}-CER mimics rituximab-induced inhibitory cell viability. Daudi cells were treated or not (○) with C_{16}-CER at 0.05 μM (●), 0.1 μM (▲), or 0.5 μM (■), and cell viability was estimated by trypan blue exclusion assay. Results are the mean of 3 independent experiments ± SD.

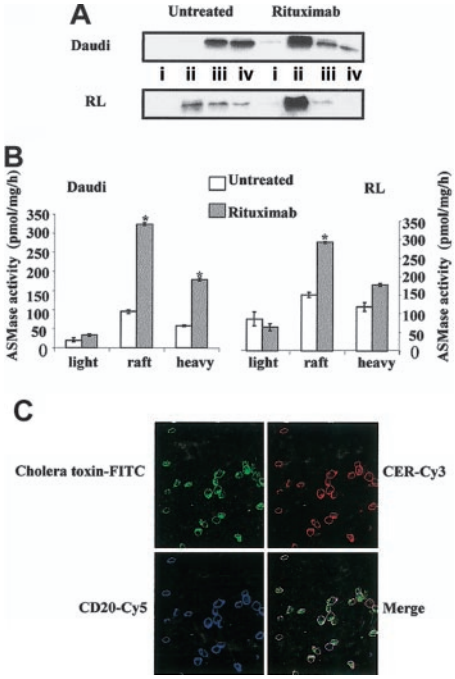

Figure 5. Rituximab induces CD20 relocalization and A-SMase activation into raft microdomains. Daudi and RL cells were treated or not for 10 minutes with 10 μg/mL rituximab, after which raft microdomains were isolated as described in "Materials and methods." (A) CD20 localization was determined by Western blot analysis using a mouse anti-CD20 antibody. (i) Light (fractions 1-3); (ii) rafts (fractions 4-6); (iii) intermediate (fractions 7-9); and (iv) heavy (fractions 10-12). (B) A-SMase activity was measured on each fraction after raft isolation as described in "Materials and methods." Results are the mean of 3 independent experiments ± SD. (C) Daudi cells were treated with 10 μg/mL rituximab for 15 minutes, then localization of CD20, CER, and raft microdomains was determined as described in "Materials and methods" by confocal microscopy.

Finally, as presented in Figure 5C, we observed that rituximab-induced CER generation is colocalized with CD20 into raft microdomains.

Role of raft microdomains on CER generation and A-SMase activation

To evaluate the role of raft microdomains in rituximab signaling, we used a cholesterol sequestering agent, methyl-β-cyclodextrin (MβCD), on CER generation and A-SMase localization after rituximab treatment. Daudi cells were preincubated with 10 mM MβCD for 30 minutes and then treated with 10 μg/mL rituximab for various times. We then evaluated the CER generation and A-SMase localization at the cell surface by flow cytometry. These experiments revealed that MβCD pretreatment resulted in total inhibition of rituximab-induced A-SMase translocation (Figure 6) and CER generation (data not shown). Moreover, our results showed that cholesterol repletion restored the A-SMase (Figure 6) translocation and CER (data not shown) accumulation at the cell surface.

Role of CER in rituximab signaling

CER has been described to trigger distinct intracellular signaling pathways, including the stimulation of ERK (p44/42 MAPK), JNK, and p38MAPK.[9-11,29,30] Therefore, we evaluated whether rituximab could activate these pathways through CER production. These experiments showed that, in both Daudi and RL cells, treatment with rituximab resulted in partial translocation of ERK proteins into raft fractions as well as ERK phosphorylation in these microdomains (Figure 7A). Moreover, SR33557 inhibits ERK

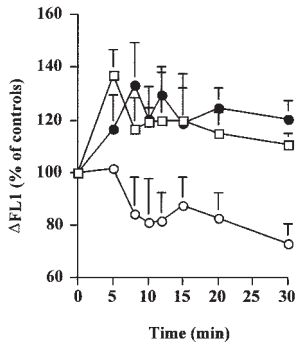

Figure 6. Raft microdomains are essential for A-SMase outer leaflet localization. Daudi cells were preincubated (○) or not (□) with methyl-β-cyclodextrin during 20 minutes at 37°C for raft disruption and then treated or not with 10 μg/mL rituximab. For cholesterol depletion-repletion experiment (●), cells were first treated with methyl-β-cyclodextrin and then incubated with cholesterol as described in "Materials and Methods." A-SMase localization was determined by FACS cytometry on nonpermeabilized cells. Results are the mean of 3 independent experiments ± SD.

phosphorylation in both Daudi and RL intact cells (Figure 7B). However, SR33557 did not significantly influence the activation of JNK and MAPK kinase 3 (MKK3), the upstream regulator of p38MAPK (data not shown). These results suggest that the CER pathway is an important functional component linking CD20 engagement and MAPK stimulation.

Previous studies have shown that CER could influence the expression of some cell cycle regulators, including p21(WAF-1) or p27(Kip1).[7,8,31] Therefore, we investigated whether the inhibition of rituximab-induced CER generation may result in p21(WAF1) and p27(Kip1) induction. In these experiments, we were unable to detect p21(WAF1) induction in rituximab-treated cells (data not shown). However, we found not only that rituximab did induce p27(Kip1) expression but also that SR33557 significantly inhibited this effect (Figure 7C).

Discussion

In this study, we show that, in Daudi and RL B-lymphoma cells, rituximab used at the saturating dose induced moderate accumulation in G_1 phase, growth inhibition, and significant loss in

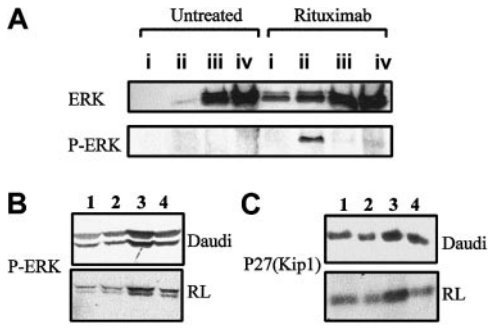

Figure 7. Rituximab induces ERK activation in raft microdomains and p27(Kip1) expression. (A) Raft microdomains of cells treated or not for 15 minutes with 10 μg/mL rituximab were isolated and then immunoblotted with antibodies recognizing ERK (p42/44 MAPK) and phospho-ERK (P-ERK). (i) Light (fractions 1-3); (ii) rafts (fractions 4-6); (iii) intermediate (fractions 7-9); and (iv) heavy (fractions 10-12). (B) Daudi and RL cells (5×10^6) were pretreated or not with 30 μM SR33557 for 1 hour, after which cells were incubated with or without 10 μg/mL rituximab for another 15 minutes. Cells were then immunoblotted with antiphospho-ERK antibody as described in "Materials and methods"; (1) untreated controls, (2) SR33557 alone, (3) rituximab alone, (4) SR33557 and rituximab. (C) Expression of p27(Kip1) was determined by Western blot analysis in Daudi and RL cells; (1) untreated controls, (2) SR33557 alone, (3) rituximab alone, (4) SR33557 and rituximab.

clonogenic potential. However, in these cells, rituximab induced no apoptosis. The antiproliferative effect of soluble forms of rituximab without apoptosis has been already reported in various cellular models, including Burkitt cells such as Daudi and Ramos.[2,32,33] Moreover, it has been also described that, whereas other malignant B cells, including most t(14;18)-positive lymphoma cell lines, displayed apoptotic features on incubation in the presence of immobilized rituximab or goat antimouse antibody $F(ab')_2$ fragments, Daudi cells were resistant.[32] Whether resistance of Daudi cells to rituximab is due to relatively low density of CD20 molecules, compared with sensitive B cells, remains uncertain because BJAB, another Burkitt cell line, is also resistant, whereas these cells exhibit high CD20 density.[34]

In this study, we show for the first time that, in vitro, treatment with rituximab may result in a rapid and transient increase in cellular CER concentration. This rituximab effect was observed in Burkitt cells as well as in most B-CLL cells. The origin of CER was also investigated. Thus, there is no evidence that CER production could be due to enhanced de novo CER synthesis. This result contrasts with BCR activation that has been found to induce CER accumulation through enhanced CER synthesis without affecting either N- or A-SMases.[13] In contrast, our study provides strong evidence that, in Daudi and RL cells, CER is produced on SM hydrolysis. Indeed, CER generation correlates with A-SMase stimulation and SM loss. Moreover, A-SMase inhibitors prevented A-SMase stimulation and CER production. This result also suggests that N-SMase is not involved in the cellular response to rituximab, whereas this enzyme has been implied in anti-IgM–induced apoptosis.[12] Previous studies have described that A-SMase can also be stimulated on γ- or UV-radiation or activation of death receptors such as Fas or p75 low-affinity nerve growth factor (NGF) receptor.[23] These observations suggest a general function of A-SMases in mediating growth inhibition or apoptosis. However, it remains unclear which A-SMase is involved in these processes. Indeed, the A-SMase gene gives rise to both lysosomal SMase and a Zn^{2+}-dependent so-called secretory A-SMase.[35] More recently, a third form of A-SMase has been detected in the detergent-resistant membrane of NIH-3T3 and PC12 cells.[36] This enzyme is Zn^{2+} independent, resides inside secretory or lysosomal vesicles, and is translocated onto the extracellular leaflet of the cell membrane on stimulation by death receptors.[25] Two lines of evidence suggest that rituximab operates through this third form of A-SMase. First, A-SMase stimulation is Zn^{2+} independent. Second, the enzyme is translocated from intracellular compartments to the cell surface. Thus, it is possible that this A-SMase subset represents a common mediator of inhibitory signals triggered by death receptors, monoclonal antibodies, and, perhaps, other antitumor agents.

The mechanism by which CD20 leads to A-SMase stimulation has not been investigated. However, it is likely that other protein components act as adaptors in this signaling complex. In this perspective, it is important to note that CD20 has been found to be associated with Src kinases, including Lyn, Fyn, and Lck, but not Blk or Bruton tyrosine kinase.[37,38] Moreover, it has been reported that anti-CD20 antibody elicits Src-mediated tyrosine phosphorylation events in normal and malignant B cells.[39-41] On the basis of the role of some Src kinases in regulating A-SMase,[42] one can speculate that these enzymes could play a role in a functional interaction between CD20 and A-SMase.

The role of CER accumulation at the external surface of the cell in the inhibition of proliferation induced by rituximab is supported by the observed inhibitory effect of C16-CER, a nonpermeant synthetic CER. This intriguing observation establishes a link between external signaling events and cell growth control machinery. As a matter of fact, A-SMase stimulation appears to be critical for ERK stimulation and p27(Kip1) induction. The role of ERK in regulating p27(Kip1) is not surprising. Indeed, previous studies have shown that ERK is, among others, an important regulator of p27(Kip1) expression.[43,44] Therefore, we propose a model in which the SM-CER pathway at least contributes to rituximab inhibitory effect through p27(Kip1). This observation may have important clinical implications. Indeed, previous studies have extensively documented that p27(Kip1) expression or distribution is frequently abnormal in lymphoid neoplasias, including advanced B-CLL, mantle cell lymphoma, or diffuse large cell lymphoma.[45-47]

To conclude, our study suggests that rituximab induced a complex signaling pathway consisting in the stimulation of an intracellular Zn^{2+}-independant A-SMase followed by the translocation of the active form of this enzyme to plasma membrane raft microdomains and hydrolysis of the outer leaflet-associated SM. CER issued from SM hydrolysis facilitates the recruitment of MAPK components in lipid microdomains and thus could be a critical intermediate of the cellular response to rituximab by linking CD20 activation and MAPK-mediated downstream effector signaling.

References

1. Maloney D-G, Smith B, Rose A. Rituximab: mechanism of action and resistance. Semin Oncol. 2002;29:2-9.
2. Ghetie M-A, Bright H, Vitetta E-S. Homodimers but not monomers of Rituxan (chimeric anti-CD20) induce apoptosis in human B-lymphoma cells and synergize with a chemotherapeutic agent and an immunotoxin. Blood. 2001;97:1392-1398.
3. Deans J-P, Li H, Polyak M-J. CD20-mediated apoptosis: signalling through lipid rafts. Immunology. 2002;107:176-182.
4. Semac I, Palomba C, Kulangara K, et al. Anti-CD20 therapeutic antibody rituximab modifies the functional organization of rafts/microdomains of B lymphoma cells. Cancer Res. 2003;63:534-540.
5. Pedersen I-M, Buhl A-M, Geisler C-H, Jurlander J. The chimeric anti-CD20 antibody rituximab induces apoptosis in B-cell chronic lymphocytic leukemia through a p38 mitogen activated protein-kinase-dependent mechanism. Blood. 2002; 99: 1314-1319.
6. Pettus B-J, Chalfant C-E, Hannun Y-A. Ceramide in apoptosis: an overview and current perspectives. Biochim Biophys Acta. 2002;1585:114-125.
7. Oh W-J, Kim W-H, Kang K-H, Kim T-Y, Kim M-Y, Choi K-H. Induction of p21 during ceramide-mediated apoptosis in human hepatocarcinoma cells. Cancer Lett. 1998;129:215-222.
8. Kim WH, Ghil KC, Lee JH, et al. Involvement of p27(Kip1) in ceramide-mediated apoptosis in HL-60 cells. Cancer Lett. 2000;151:39-48.
9. Subbaramaiah K, Chung W-J, Dannenberg A-J. Ceramide regulates the transcription of cyclooxygenase-2. Evidence for involvement of extracellular signal-regulated kinase/c-Jun N-terminal kinase and p38 mitogen-activated protein kinase pathways. J Biol Chem. 1998;273:32943-32949.
10. Verheij M, Bose R, Lin XH, et al. Requirement for ceramide-initiated SAPK/JNK signalling in stress-induced apoptosis. Nature. 1996;380:75-79.
11. Brenner B, Koppenhoefer U, Weinstock C, Linderkamp O, Lang F, Gulbins E. Fas- or ceramide-induced apoptosis is mediated by a Rac1-regulated activation of Jun N-terminal kinase/p38 kinases and GADD153. J Biol Chem. 1997;272: 22173-22181.
12. Wiesner D-A, Kilkus J-P, Gottschalk A-R, Quintans J, Dawson G. Anti-immunoglobulin-induced apoptosis in WEHI 231 cells involves the slow formation of ceramide from sphingomyelin and is blocked by bcl-XL. J Biol Chem. 1997;272:9868-9876.
13. Kroesen BJ, Pettus B, Luberto C, et al. Induction of apoptosis through B-cell receptor cross-linking occurs via de novo generated C16-ceramide and involves mitochondria. J Biol Chem. 2001;276: 13606-13614.
14. Levade T, Jaffrézou J-P. Signalling sphingomyelinases: which, where, how and why? Biochim Biophys Acta. 1999;1438:1-17.
15. Lisanti M-P, Tang Z, Scherer P-E, Sargiacomo M. Caveolae purification and glycosylphosphatidylinositol-linked protein sorting in polarized epithelia. Methods Enzymol. 1995;250:655-668.

16. Smith PK, Krohn RI, Hermanson GT, et al. Measurement of protein using bicinchoninic acid [erratum appears in Anal Biochem. 1987;163:279]. Anal Biochem. 1985;150:76-85.
17. Jaffrézou JP, Levade T, Bettaieb A, et al. Daunorubicin-induced apoptosis: triggering of ceramide generation through sphingomyelin hydrolysis. EMBO J. 1996;15:2417-2424.
18. Wiegmann K, Schutze S, Machleidt T, Witte D, Kronke M. Functional dichotomy of neutral and acidic sphingomyelinases in tumor necrosis factor signaling. Cell. 1994; 78:1005-1015.
19. Andrieu N, Salvayre R, Levade T. Evidence against involvement of the acid lysosomal sphingomyelinase in the tumor-necrosis-factor- and interleukin-1-induced sphingomyelin cycle and cell proliferation in human fibroblasts. Biochem J. 1994;303:341-345.
20. Van Veldhoven P-P, Matthews T-J, Bolognesi D-P, Bell R-M. Changes in bioactive lipids, alkylacylglycerol and ceramide, occur in HIV-infected cells. Biochem Biophys Res Commun. 1992;187: 209-216.
21. Cuvillier O, Edsall L, Spiegel S. Involvement of sphingosine in mitochondria-dependent Fas-induced apoptosis of type II Jurkat T cells. J Biol Chem. 2000;275:15691-15700.
22. Jaffrézou J-P, Maestre N, de Mas-Mansat V, Bezombes C, Levade T, Laurent G. Positive feedback control of neutral sphingomyelinase activity by ceramide. FASEB J. 1998;12:999-1006.
23. Jaffrézou J-P, Herbert J-M, Levade T, Gau M-N, Chatelain P, Laurent G. Reversal of multidrug resistance by calcium channel blocker SR33557 without photoaffinity labeling of P-glycoprotein. J Biol Chem. 1991;266:19858-19864.
24. Jaffrezou J-P, Levade T, Chatelain P, Laurent G. Modulation of subcellular distribution of doxorubicin in multidrug-resistant P388/ADR mouse leukemia cells by the chemosensitizer ((2-isopropyl-1-(4-[3-N-methyl-N-(3,4-dimethoxy-beta-phenethyl) amino]propyloxy)-benzenesulfonyl)) indolizine. Cancer Res. 1992;52:6440-6446.
25. Gulbins E, Grassme H. Ceramide and cell death receptor clustering. Biochem Biophys Acta. 2002; 1585:139-145.
26. Grassme H, Jendrossek V, Bock J, Riehle A, Gulbins E. Ceramide-rich membrane rafts mediate CD40 clustering. J Immunol. 2002;168:298-307.
27. Grassme H, Schwarz H, Gulbins E. Molecular mechanisms of ceramide-mediated CD95 clustering. Biochem Biophys Res Commun. 2001;284: 1016-1030.
28. Chan CHT, Hughes D, French RR, et al. CD20-induced lymphoma cell death is independent of both capsases and its redistribution into Triton X-100 insoluble membrane rafts. Cancer Res. 2003;63:5480-5489.
29. Maziere C, Conte M-A, Maziere J-C. Activation of the JAK/STAT pathway by ceramide in cultured human fibroblasts. FEBS Lett. 2001;507:163-168.
30. Willaime S, Vanhoutte P, Caboche J, Lemaigre-Dubreuil Y, Mariani J, Brugg B. Ceramide-induced apoptosis in cortical neurons is mediated by an increase in p38 phosphorylation and not by the decrease in ERK phosphorylation. Eur J Neurosci. 2001;13:2037-2046.
31. Alesse E, Zazzeroni F, Angelucci A, Giannini G, Di Marcotullio L, Gulino A. The growth arrest and downregulation of c-myc transcription induced by ceramide are related events dependent on p21 induction, Rb underphosphorylation and E2F sequestering. Cell Death Differ. 1998;5:381-389.
32. Flieger D, Renoth S, Beier I, Sauerbruch T, Schlidt-Wolf I. Mechanism of cytotoxicity induced by chimeric mouse human monoclonal antibody IDEC-C2B8 in CD20-expressing lymphoma cell lines. Cell Immunol. 2000;204:55-63.
33. Cardarelli PM, Quinn M, Buckman D, et al. Binding to CD20 by anti-B1 antibody or $F(ab')_2$ is sufficient for induction of apoptosis in B-cell lines. Cancer Immunol Immunother. 2002;51:15-24.
34. Mathas S, Rickers A, Bommert K, Dörken B, Mapara M-Y. Anti-CD20 and B cell receptor-mediated apoptosis: evidence for shared intracellular signalling pathways. Cancer Res. 2000;60:7170-7176.
35. Schissel S-L, Keesler G-A, Schuchman E-H, Williams K-J, Tabas I. The cellular trafficking and zinc dependence of secretory and lysosomal sphingomyelinase, two products of the acid sphingomyelinase gene. J Biol Chem. 1998;273: 18250-18259.
36. Dobrowsky R-T, Gazula V-R. Analysis of sphingomyelin hydrolysis in caveolar membranes. Methods Enzymol. 2000;311:184-193.
37. Deans J-P, Kalt L, Ledbetter J-A, Schieven G-L, Bolen J-B, Johnson P. Association of 75/80 kDa phosphoproteins and the tyrosine kinases Lyn, Fyn, and Lck with the B cell molecule CD20. Evidence against the involvement of the cytoplasmic regions of CD20. J Biol Chem. 1995;270:22632-22638.
38. Popoff I-J, Savage J-A, Blake J, Johnson J, Deans J-P. The association between CD20 and Scr-family tyrosine kinases requires an additional factor. Mol Immunol. 1998;35:207-214.
39. Deans JP, Schieven GL, Shu GL, et al. Association of tyrosine and serine kinases with the B cell surface antigen CD20. Induction via CD20 of tyrosine phosphorylation and activation of phospholipase C-gamma 1 and PLC phospholipase C-gamma 2. J Immunol. 1993;151:4494-4504.
40. Shan D, Ledbetter J-A, Press O-W. Signaling events involved in anti-CD20-induced apoptosis of malignant human B cells. Cancer Immunol Immunother. 2000;48:673-683.
41. Hofmeister J-K, Cooney D, Coggeshall K-M. Clustered CD20 induced apoptosis: Src-family kinase, the proximal regulator of tyrosine phosphorylation, calcium influx, and caspases 3-dependent apoptosis. Blood Cells Mol Dis. 2000;26: 133-143.
42. Marchetti M-C, Di Marco B, Cifone G, Migliorati G, Riccardi C. Dexamethasone-induced apoptosis of thymocytes: role of glucocorticoid receptor-associated Src kinase and caspase-8 activation. Blood. 2003;101:585-593.
43. Ray R-M, Zimmerman B-J, McCormack S-A, Patel T-B, Johnson L-R. Polyamine depletion arrests cell cycle and induces inhibitors p21(Waf1/Cip1), p27(Kip1), and p53 in IEC-6 cells. Am J Physiol. 1999;276:684-691.
44. Das D, Pintucci G, Stern A. MAPK-dependent expression of p21(WAF) and p27(kip1) in PMA-induced differentiation of HL60 cells. FEBS Lett. 2000;472:50-52.
45. Cobo F, Martinez A, Pinyol M, et al. Multiple cell cycle regulator alterations in Richter's transformation of chronic lymphocytic leukemia. Leukemia. 2002;16:1028-1034.
46. Chiarle R, Budel LM, Skolnik J, et al. Increased proteasome degradation of cyclin-dependent kinase inhibitor p27 is associated with a decreased overall survival in mantle cell lymphoma. Blood. 2000;95:619-626.
47. Saez A, Sanchez E, Sanchez-Beato M, et al. p27KIP1 is abnormally expressed in diffuse large B-cell lymphomas and is associated with an adverse clinical outcome. Br J Cancer. 1999;80: 1427-1434.